

Reaction of Cl with CD₄ excited to the second C–D stretching overtone

Marion R. Martin, Davida J. Ankeny Brown, Albert S. Chiou, and Richard N. Zare
Department of Chemistry, Stanford University, Stanford, California 94305-5080

(Received 1 November 2006; accepted 11 December 2006; published online 30 January 2007)

The effects of vibrational excitation on the Cl+CD₄ reaction are investigated by preparing three nearly isoenergetic vibrational states: |3000⟩ at 6279.66 cm⁻¹, |2100⟩ at 6534.20 cm⁻¹, and |1110⟩ at 6764.24 cm⁻¹, where |D₁D₂D₃D₄⟩ identifies the number of vibrational quanta in each C–D oscillator. Vibrational excitation of the perdeuteromethane is via direct infrared pumping. The reaction is initiated by photolysis of molecular chlorine at 355 nm. The nascent methyl radical product distribution is measured by 2+1 resonance-enhanced multiphoton ionization at 330 nm. The resulting CD₃ state distributions reveal a preference to remove all energy available in the most excited C–D oscillator. Although the energetics are nearly identical, the authors observe strong mode specificity in which the CD₃ state distributions markedly differ between the three Cl-atom reactions. Reaction with CD₄ prepared in the |3000⟩ mode leads to CD₃ products populated primarily in the ground state, reaction with CD₄ prepared in the |2100⟩ mode leads primarily to CD₃ with one quantum of stretch excitation, and reaction with CD₄ prepared in the |1110⟩ mode leads primarily to CD₃ with one quantum of C–D stretch excitation in two oscillators. There are some minor deviations from this behavior, most notably that the Cl atom is able to abstract more energy than is available in a single C–D oscillator, as in the case of |2100⟩, wherein a small population of ground-state CD₃ is observed. These exceptions likely result from the mixings between different second overtone stretch combination bands. They also measure isotropic and anisotropic time-of-flight profiles of CD₃ ($\nu_1=1, 2$) products from the Cl+CD₄ |2100⟩ reaction, providing speed distributions, spatial anisotropies, and differential cross sections that indicate that energy introduced as vibrational energy into the system essentially remains as such throughout the course of the reaction. © 2007 American Institute of Physics. [DOI: [10.1063/1.2431368](https://doi.org/10.1063/1.2431368)]

I. INTRODUCTION

Vibrational control of reactions has been of long-standing interest. This process was first demonstrated in the reaction of H+HOD.^{1–4} The H-atom abstraction channel is favored when the OH bond is vibrationally excited, whereas preparing OD stretching opens the D-atom abstraction channel. Similar results were reported on Cl+HOD.⁵ The vibrational excitation of the products directly reflects the vibrational wave function of the excited molecule. A spectator model was proposed to explain this behavior, wherein the unexcited part of the molecule does not play a role in influencing the outcome of the reaction.

In the Cl+CH₄→HCl+CH₃ reaction, excitation of the ν_3 antisymmetric stretch of CH₄ enhances the reaction by a factor of 30±15,⁶ and the reactivity enhancement is localized in the C–H bond that is excited.⁷ This result is of particular interest as the fundamental vibrational transition is typically viewed as a normal mode vibration, in which all the atoms in the molecule move in a concerted motion at a certain frequency while the center of mass of the molecule remains stationary.⁸ Only in the overtone region, where large bond anharmonicity begins to quench the interbond coupling, would one expect the vibration to take on more local mode character, where the stretching motion is isolated in single C–H oscillators.⁹ In the Cl+CH₄ ($\nu_3=1$) reaction, it appears that a local mode picture better explains the observed reactivity. Interactions between the approaching Cl atom and the

vibrational wave function of methane perturb the normal mode wave function so that the Cl atom reacts with a single excited C–H oscillator^{10,11} and the remainder of the methane molecule is left in the ground state, just as predicted by the spectator model.

Further study of the Cl+methane reaction has provided support for this model, where strong mode specificity and bond selectivity have been observed. In the reactions of Cl with methane (CH₂D₂ and CHD₃) excited to its first C–H stretch overtone, only the activated C–H bond takes part in the reaction, and the initial vibrational motion of the methane reagent appears not to be redistributed through the course of the reaction.⁷ Kim *et al.*¹² investigated the reaction of Cl with CH₄ excited into the first overtone of the antisymmetric stretch, where CH₄ can be prepared, via direct IR absorption, to have one quantum of stretch in two C–H oscillators, |1100⟩. The local mode notation |H₁H₂H₃H₄⟩ indicates the bond excitation state for each of the C–H oscillators. The majority of the methyl radical products are stretch excited, with the remainder being formed with some energy in the bending motion. Bechtel *et al.*¹³ studied the reaction of Cl with CD₄ excited in the first overtone region and found very similar results. Holiday *et al.*¹⁴ studied the reaction of Cl with CH₃D excited into three C–H stretch overtones near 6000 cm⁻¹: |110⟩ |0⟩, |200⟩ |0⟩, and |100⟩ |0⟩ + $\nu_3+\nu_5$. The observed bond and mode selectivity, as well as the CH₂D internal state distributions, are best accounted for using a

local mode description of the vibrational motion along with a spectator model for the Cl reactivity. We proposed that a study of reactions of Cl with CH_4 and its isotopomers excited into higher stretch overtones would be of interest in testing the validity of the spectator stripping model. We would expect that at some point vibrational redistribution will become so important that purely statistical behavior would begin to dominate over local mode behavior.

Studying the reaction of Cl with CD_4 excited in the second overtone stretching region has yielded interesting results. Owing to the possible stretch combinations, we can prepare three different vibrational motions with direct IR excitation: $|3000\rangle$, $|2100\rangle$, and $|1110\rangle$. These vibrations have very similar energies but quite different motions. Resonance-enhanced multiphoton ionization (REMPI) spectra have been taken for the reaction of Cl with CD_4 excited into each of these modes, where distinctive CD_3 integral cross sections are measured for each vibrational motion. The results for second overtone excitation of the C–D stretch in CD_4 continue to follow closely the predictions of the spectator stripping model.

II. EXPERIMENT

A. Experimental apparatus

The experimental apparatus has been described in detail elsewhere,¹⁵ therefore only the most important features are described here. A 1:4:7 mixture of molecular chlorine (Cl_2 : Matheson, research grade: 99.999%), perdeuteromethane (CD_4 : Cambridge, 98%), and helium (He: Liquid Carbonic, 99.995%) is supersonically expanded into the extraction region of a Wiley-McLaren time-of-flight (TOF) spectrometer¹⁶ under single-collision conditions. The vibrational state of methane is prepared by direct IR excitation at $\sim 1.5 \mu\text{m}$. The reaction is initiated by the photolysis of Cl_2 with linearly polarized 355 nm light, which produces monoenergetic Cl atoms primarily in the ground state (${}^2P_{3/2}$) with a spatial anisotropy, $\beta = -1$.¹⁷ After a 20–100 ns time delay for the reaction to occur, the CD_3 products are state selectively ionized by 2+1 REMPI through the $3p$ Rydberg state^{18,19} and detected by microchannel plates. The reactive signal from vibrationally excited methane is separated from the ground-state reactive signal by turning the IR light off and on and subtracting the resultant signals on a shot-by-shot basis.

The IR radiation required to prepare the vibrational states of CD_4 in the second overtone stretching region is generated in a two-step process involving difference-frequency mixing (DFM) and optical parametric amplification (see Fig. 1). Tunable IR light between 1.47 and 1.61 μm is first generated by DFM by combining the 1.064 μm fundamental of a Nd^{3+} :YAG (yttrium aluminum garnet) laser (Continuum, PL9020) with the output of a Nd^{3+} :YAG (Continuum, PL9020) pumped dye laser (Continuum, ND6000; Exciton, DCM) in a beta barium borate (BBO) crystal. The near-IR radiation is then combined with a 532 nm beam in a BBO crystal to produce approximately 30 mJ of radiation. The IR bandwidth is $\sim 1 \text{ cm}^{-1}$. The photolysis source at 355 nm is the third harmonic of a Nd^{3+} :YAG laser (Con-

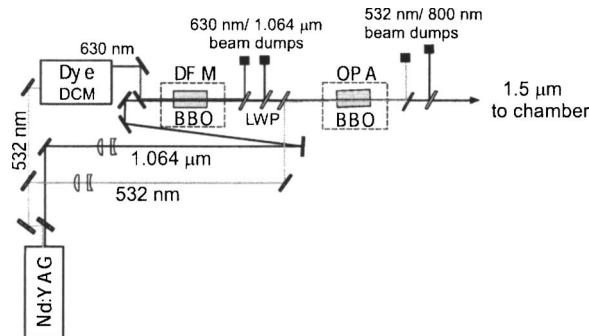


FIG. 1. Schematic of IR light generation. A long wave pass (LWP) filter is used to separate the 1.064 μm light from the 1.5 μm light.

tinuum, PL8020). The probe laser beam at approximately 330 nm is generated by doubling the output of a dye laser (Lambda Physik, FL2002; Exciton, DCM/LDS698 mix) pumped by a third Nd^{3+} :YAG laser (Spectra Physics, DCR-2A). We concentrated on the $3p\ {}^2A_2^{\prime\prime} 0_0^0$, 1_1^1 , and 1_2^2 vibronic bands in CD_3 .²⁰ Here the label “l” represents the ν_1 symmetric stretch vibrational manifold, while the subscript and the superscript indicate the vibrational quantum number in the ground $2p\ {}^2A_2^{\prime\prime}$ and the intermediate $3p\ {}^2A_2^{\prime\prime}$ electronic excited states, respectively.^{18,19}

A photoelastic modulator (PEM-80, Hinds International, Inc.) flips the linear polarization direction of the photolysis laser between parallel and perpendicular to the TOF axis on an every-other-shot basis, providing the isotropic $I_{\text{iso}} = I_{\parallel} + 2I_{\perp}$ and anisotropic $I_{\text{aniso}} = 2(I_{\parallel} - I_{\perp})$ components of the core-extracted TOF profiles. The isotropic TOF profile removes any dependence on the spatial anisotropy, allowing for direct measurement of the speed distribution. The anisotropic TOF profile is used to estimate the amount of coproduct internal energy by a method described in previous publications.^{12,15} With this approximation of the internal energy of the coproducts, the isotropic TOF profiles are analyzed and converted into differential cross sections (DCSs) using a method similar to that of Simpson *et al.*¹⁵

B. Infrared spectroscopy of perdeuteromethane (CD_4)

The CD_4 absorption spectrum was measured in the 900–8500 cm^{-1} region by Kaylor and Nielsen.²¹ They make assignments to the three IR active stretch-only combinations in the second overtone stretching region: $2\nu_1 + \nu_3$, $\nu_1 + 2\nu_3$, and $3\nu_3$. Photoacoustic spectra taken in this laboratory of the regions Kaylor and Nielsen assigned as stretch-only combinations as well as an unassigned band agree well with the absorption spectrum presented in their paper. The action spectra of this same region are shown in Fig. 2, where CD_3 ($\nu_1=1$ or $\nu_1=2$) from the reaction of Cl with CD_4 excited by direct IR excitation are measured. The difference in signal to noise ratio in these scans arises from the differences in the absorption cross sections of these vibrational modes.

Halonen and Child⁹ have developed a local mode model to describe the vibration of tetrahedral molecules, where a three parameter coupled Morse oscillator model fitted to available spectroscopic data is applied to predict vibrational

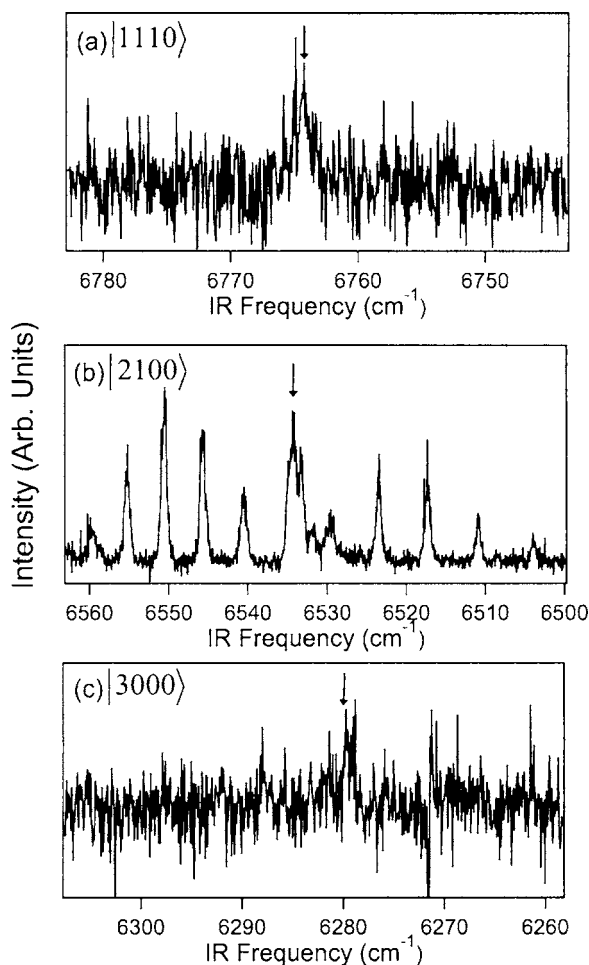


FIG. 2. Action spectra obtained by scanning the IR laser frequency over the second stretching overtone region while using REMPI to monitor the CD₃ ($\nu_1=1$ or $\nu_1=2$) products of the reaction of Cl with: (a) CD₄|1110⟩ to give CD₃ ($\nu_1=2$), (b) CD₄|2100⟩ to give CD₃ ($\nu_1=1$), and (c) CD₄|3000⟩ to give CD₃ ($\nu_1=1$). The arrows indicate the IR laser wavelengths used for measuring the integral cross sections for each of the three reactions.

energies in the stretching overtone bands with total quantum number $\nu \leq 5$. In a normal mode picture of molecular vibration, interbond coupling distributes the vibrational energy equally throughout the molecule, causing the bonds to oscillate with the same frequency. In contrast, each bond is seen as an isolated oscillator in the local mode view, where bond anharmonicity dominates. Halonen and Child⁹ vary the ratio of bond anharmonicity to interbond coupling strength to map from a normal to local mode picture, where the $2\nu_1+\nu_3$, $\nu_1+2\nu_3$, and $3\nu_3$ modes correspond to |3000⟩, |2100⟩, and |1110⟩, respectively. Each of these modes has F_2 symmetry and is IR active. Halonen and Child also use the bond anharmonicity to interbond coupling strength ratio for a particular molecule to predict whether it will have more local or normal mode character; CD₄ has a ratio of about 0.7, indicating slight harmonic nature. By comparison, the ratio is about 2 for CH₄, which is more local in nature.⁹ Based on the photoacoustic data, action spectra, and previous theoretical and experimental work, the REMPI spectra are taken at the following line positions: 6279.66 cm⁻¹ as |3000⟩, 6534.20 cm⁻¹ as |2100⟩, and 6764.24 cm⁻¹ as |1110⟩.

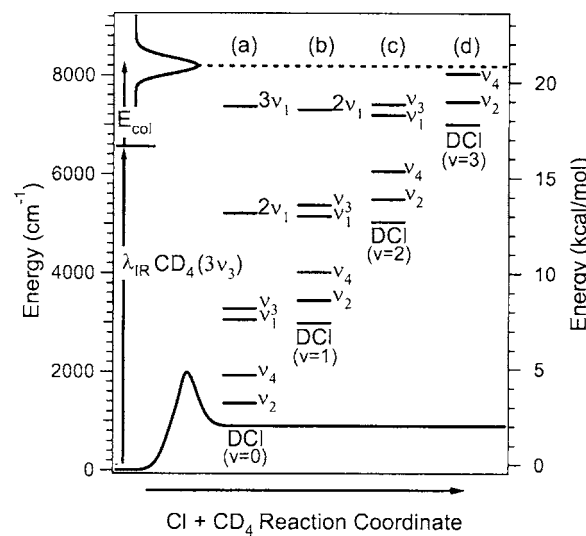


FIG. 3. Energetics of the Cl+CD₄ reaction. Channels (a)–(d) correspond to possible internal energy product distributions, where the CD₃ vibrational states are superimposed on the DCI vibrational energy levels. The CD₃ vibrational modes are the symmetric stretch ($\nu_1=2158\text{ cm}^{-1}$), the umbrella bend ($\nu_2=458\text{ cm}^{-1}$), the antisymmetric stretch ($\nu_3=2381\text{ cm}^{-1}$), and the deformation ($\nu_4=1027\text{ cm}^{-1}$). The collisional energy spread is represented by a Gaussian distribution generated using the formulas of van der Zande *et al.* (Ref. 23) assuming a translational temperature of 10 K.

C. Energetics

Figure 3 displays the relevant energetics of the Cl+CD₄ reaction. This reaction is slightly endothermic, $\Delta H = 900\text{ cm}^{-1}$ (2.6 kcal mol⁻¹, 0.11 eV). The *ab initio* barrier height is $\sim 2200\text{ cm}^{-1}$ (6.4 kcal mol⁻¹, 0.27 eV).²² Photolysis of Cl₂ at 355 nm provides $1490 \pm 150\text{ cm}^{-1}$ (0.18 \pm 0.02 eV) of translational energy in the center-of-mass frame, assuming a translational temperature of 10 K for the pulsed expansion.²³ Excitation of the stretching overtone provides an additional $6280\text{--}6760\text{ cm}^{-1}$ of energy, giving a total energy, $\sim 8250\text{ cm}^{-1}$ (1.02 eV), that is well above the reaction threshold. Figure 3 also displays the energetically allowed vibrational states of the product, where the CD₃ vibrational modes are the symmetric stretch ($\nu_1=2158\text{ cm}^{-1}$), the umbrella bend ($\nu_2=458\text{ cm}^{-1}$), the antisymmetric stretch ($\nu_3=2381\text{ cm}^{-1}$), and the deformation ($\nu_4=1027\text{ cm}^{-1}$). There is enough energy to populate up to the CD₃ ($\nu_1=3$) vibrational level, with the remaining energy available for either DCI internal excitation or translational motion of both products. As shown below, the reactions of Cl with CD₄ prepared in these stretching motions have essentially the same total energy, with the difference not being much more than the spread in translational energy that arises from photolysis of Cl₂ at 355 nm.



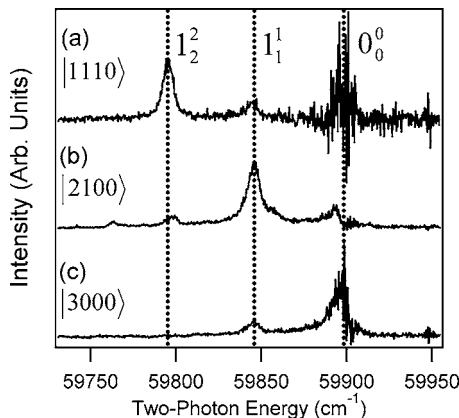


FIG. 4. 2+1 REMPI spectra of the CD_3 products from the reaction of Cl with (a) $\text{CD}_4|1110\rangle$, (b) $\text{CD}_4|2100\rangle$, and (c) $\text{CD}_4|3000\rangle$. CD_3 band assignments are also shown, where the label “1” represents the ν_1 symmetric stretch vibrational manifold, while the subscript and the superscript indicate the vibrational quantum number in the ground $3p\ ^2A''_2$ and the intermediate $3p\ ^2A''_2$ electronic excited states, respectively.

III. RESULTS AND DISCUSSION

The spectator model for reactions of Cl with CD_4 , along with the local mode picture for vibrations in CD_4 , predicts that Cl-atom reactions with $\text{CD}_4|3000\rangle$ will form CD_3 radicals primarily in the ground state, the CD_3 products from the $\text{Cl}+\text{CD}_4|2100\rangle$ reaction will form with either one quantum or two quanta of C-D stretch excitation, and, finally, the CD_3 products from the $\text{Cl}+\text{CD}_4|1110\rangle$ reaction will form with one quantum each in two C-D stretch-excited modes.

Figure 4 shows the CD_3 integral cross sections measured by REMPI. The measured product distributions match the predictions quite closely. Although the different unknown predissociation rates from the $3p\ ^2A''_2$ intermediate state^{19,24} for the CD_3 products prevent an absolute comparison of the internal state populations, it is clear that exciting each mode leads to a distinctive CD_3 product distribution. We observe a preference to remove all energy available in the most excited C-D oscillator with a few minor deviations. Exciting the $|3000\rangle$, $|2100\rangle$, or $|1110\rangle$ mode leads to CD_3 products populated primarily in the ground state, in a state with one quantum of stretch excitation, or in a state with two quanta of stretch excitation, respectively. Based on the spectator model, we would also expect that antisymmetric stretch-excited CD_3 ($\nu_3=1, 2$, or 3) products would be formed, but are unable to identify or rule out these products because the CD_3 (ν_3) mode has not been observed in any CD_3 2+1 REMPI spectrum.

It is interesting to note that although the predictions for the major product channels hold true, other product channels are accessed in the $\text{Cl}+\text{CD}_4$ reactions. The $\text{Cl}+\text{CD}_4|3000\rangle$ reaction produces some CD_3 with one quantum of stretch excitation. In the case of the $\text{Cl}+\text{CD}_4|2100\rangle$ reaction, CD_3 products formed in the ground state or with two or three quanta of stretch excitation are observed. The $\text{Cl}+\text{CD}_4|1110\rangle$ reaction produces CD_3 with one quantum of stretch excitation and maybe some ground-state CD_3 formed, but large backgrounds from the ground-state reaction prevent a definitive statement on the presence of the ground-state radical. Nonetheless, these other product channels are most

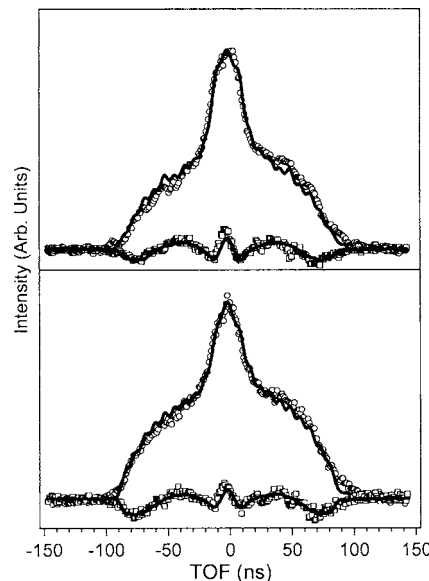


FIG. 5. Isotropic (open circles) and anisotropic (open squares) TOF profiles of the products from the $\text{Cl}+\text{CD}_4|2100\rangle$ reaction: CD_3 ($\nu_1=1$) (upper panel) and CD_3 ($\nu_1=2$) (lower panel). The thick, solid line is the result of the fit.

likely accessed because these vibrational states are highly mixed states, with rather strong coupling between the states due to the slight harmonic nature of CD_4 . The Cl atom also perturbs to some extent the vibrational wave function as it approaches a molecule to react with the most highly excited C-D bond,^{10,11} which may further mix the vibrational state.

Figure 5 shows the isotropic and anisotropic core-extracted TOF profiles measured for the CD_3 ($\nu_1=1, 2$) products from the $\text{Cl}+\text{CD}_4|2100\rangle$ reaction. The TOF measurements show little dependence on the CD_3 internal energy. Figure 6 shows the speed distributions obtained by fitting the isotropic TOF profiles. Fitting the anisotropic TOF profiles yields measurements of the product speed-dependent spatial anisotropy, which are shown in Fig. 7 with calculated curves

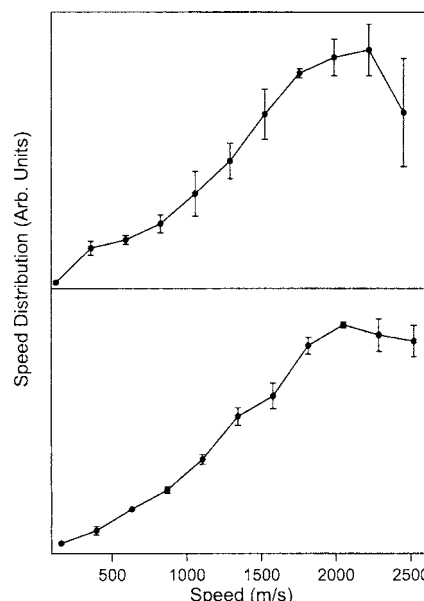


FIG. 6. Speed distributions of the products from the $\text{Cl}+\text{CD}_4|2100\rangle$ reaction: CD_3 ($\nu_1=1$) (upper panel) and CD_3 ($\nu_1=2$) (lower panel).

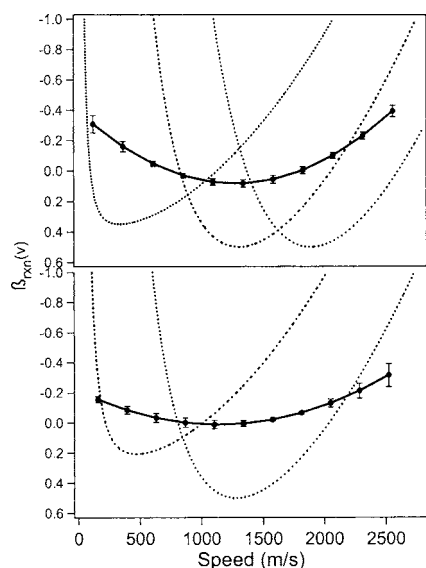
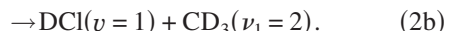
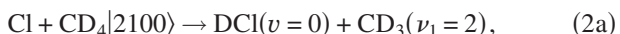


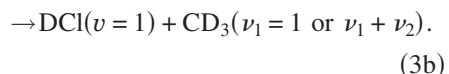
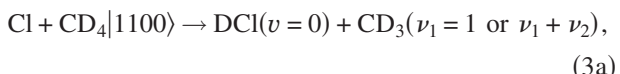
FIG. 7. Spatial anisotropy measurements of the products from the Cl + CD₄[2100] reaction: CD₃ ($\nu_1=1$) (upper panel) and CD₃ ($\nu_1=2$) (lower panel). The thick, solid lines with filled circles represent the experimental values and the remaining curves are calculated assuming various degrees of DCI internal energy: DCI ($v=0$) (dashed line), DCI ($v=1$) (dash-dot line), or DCI ($v=2$) (dotted line).

that correspond to varying levels of internal energy deposited in the DCI coproduct. The speed distributions for the two CD₃ products agree within our experimental error. The spatial anisotropy measurements do not agree as well, but this is most likely caused by the different internal energy distributions of the DCI products formed with the CD₃ ($\nu_1=1$) or CD₃ ($\nu_1=2$). These measurements indicate that the large majority of energy introduced to the system as vibrational energy remains as such in the CD₃ or DCI products and is not converted into translational energy.

We are able to investigate in more detail the CD₃ ($\nu_1=2$) products from the reaction of Cl with CD₄ [2100], which arises from two possible channels based on the energetics of the reaction



Based on the spectator stripping model, these channels are analogous to two major product channels identified by Bechtel *et al.*¹³ in their work,



From the measured spatial anisotropy, the speed distribution of CD₃ ($\nu_1=2$) is decomposed into contributions from the two channels [see Fig. 8(a)]. The low-speed component of CD₃ ($\nu_1=2$) is mostly produced with DCI ($v=1$) and the high-speed one corresponds to the DCI ($v=0$). These speed distributions are analyzed to give the DCSs for CD₃ ($\nu_1=2$) formed with DCI ($v=0$ or 1) [see Figs. 8(b) and 8(c)].

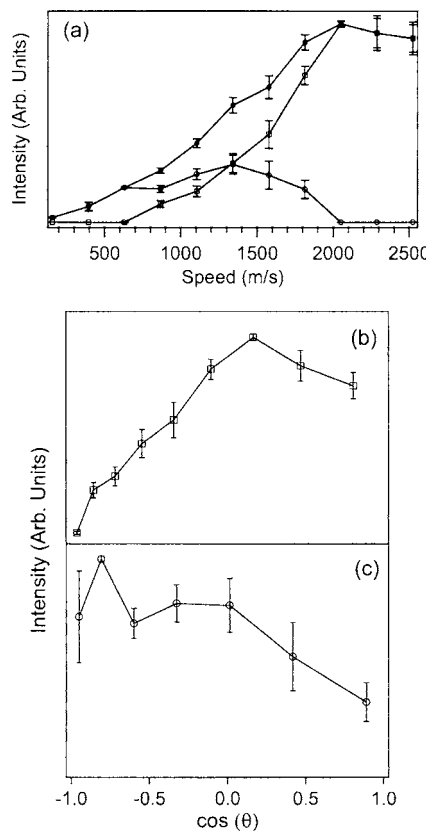


FIG. 8. (a) Speed distribution of CD₃ ($\nu_1=2$) (closed circles) and deconvolution into two subchannel contributions: DCI ($v=0$) (open squares) and DCI ($v=1$) (open circles). (b) DCS of CD₃ ($\nu_1=2$) formed with DCI ($v=0$). (c) DCS of CD₃ ($\nu_1=2$) formed with DCI ($v=1$).

The CD₃ products from channel (2a) are largely forward scattered, whereas the CD₃ products formed from channel (2b) are slightly backward scattered. These findings agree well with those of Bechtel *et al.*¹³ who found that the DCI products from channel (3a) are largely backscattered and those from channel (3b) are slightly forward scattered. A hard-sphere scattering model^{12,13} was modified to include an impulsive release ($\Delta E/E_0$) along the line of centers (IR-LOC), where the E_0 is the initial collision energy and ΔE is the kinetic energy release upon contact. This model makes two assumptions: (1) direct, localized reactivity of the polyatomic reagent and (2) a narrow cone of acceptance around the reactive bond. The IR-LOC model qualitatively describes the observed dynamics of the Cl+CH₄/CD₄ [1100] reactions^{12,13} and, by analogy, the Cl+CD₄ [2100] reaction.

IV. CONCLUSIONS

We have measured the CD₃ product state distributions in the reaction of Cl with CD₄ excited into a stretch combination band in the second overtone stretching region. A local mode description of vibrational motion in the CD₄ molecule describes well the observed CD₃ products, where the Cl atom predominantly reacts with the most stretch-excited C–D bond. This reaction is an excellent example of mode specificity, where the outcome of the reaction is determined by the vibrational motion of the CD₄ rather than by the total energy available to overcome the reaction barrier and subse-

quently access reactive channels along the reaction coordinate. Accordingly, we see three unique methyl product distributions coinciding with the three different stretching motions that are excited: $|3000\rangle$, $|2100\rangle$, and $|1110\rangle$. We also observe TOF profiles, speed distributions, spatial anisotropies, and DCSs that indicate that energy introduced as vibrational energy into the system essentially remains as such throughout the course of the reaction. Mode specificity is observed when the following conditions are met: (1) the vibrational motion is localized, (2) the reaction is direct and occurs more rapidly than vibrational redistribution, and (3) the vibrational motion prepared in the reagent has a large projection on the reaction coordinate.⁷ Evidently, the Cl-atom reaction with CD_4 excited to the second overtone of its C–D stretch satisfies well these three conditions.

ACKNOWLEDGMENTS

One of the authors (M.R.M.) thanks the National Science Foundation for a graduate fellowship, the National Football Foundation and College Hall of Fame for a scholar-athlete award, the Ford Foundation Diversity Fellowships for a dissertation award, and the Leadership Alliance for a Schering-Plough fellowship. The authors thank Jon P. Camden and Hans A. Bechtel for useful discussions. This work was supported by National Science Foundation Grant No. 0242103.

¹A. Sinha, M. C. Hsiao, and F. F. Crim, J. Chem. Phys. **94**, 4928 (1991).

²M. C. Hsiao, A. Sinha, and F. F. Crim, J. Chem. Phys. **95**, 8263 (1991).

³M. J. Bronikowski, W. R. Simpson, and R. N. Zare, J. Phys. Chem. **97**, 2194 (1993).

- ⁴M. J. Bronikowski, W. R. Simpson, B. Girard, and R. N. Zare, J. Chem. Phys. **95**, 8647 (1991).
- ⁵A. Sinha, J. D. Thoemke, and F. F. Crim, J. Chem. Phys. **96**, 372 (1992).
- ⁶W. R. Simpson, T. P. Rakitzis, S. A. Kandel, T. Lev-On, and R. N. Zare, J. Phys. Chem. **100**, 7938 (1996).
- ⁷Z.-H. Kim, H. A. Bechtel, and R. N. Zare, J. Am. Chem. Soc. **123**, 12714 (2001).
- ⁸G. Herzberg, *Infrared and Raman Spectra of Polyatomic Molecules* (Van Nostrand, New York, 1945).
- ⁹L. Halonen and M. S. Child, Mol. Phys. **46**, 239 (1982).
- ¹⁰J. P. Camden, H. A. Bechtel, D. J. A. Brown, and R. N. Zare, J. Chem. Phys. **123**, 134301 (2005).
- ¹¹S. Yoon, R. J. Holiday, E. L. Sibert, and F. F. Crim, J. Chem. Phys. **119**, 9568 (2003).
- ¹²Z.-H. Kim, H. A. Bechtel, and R. N. Zare, J. Chem. Phys. **117**, 3232 (2002).
- ¹³H. A. Bechtel, Z.-H. Kim, J. P. Camden, and R. N. Zare, Mol. Phys. **103**, 1837 (2005).
- ¹⁴R. J. Holiday, C. H. Kwon, C. J. Annesley, and F. F. Crim, J. Chem. Phys. **125**, 133101 (2006).
- ¹⁵W. R. Simpson, A. J. Orr-Ewing, T. P. Rakitzis, S. A. Kandel, and R. N. Zare, J. Chem. Phys. **103**, 7299 (1995).
- ¹⁶W. C. Wiley and I. H. McLaren, Rev. Sci. Instrum. **26**, 1150 (1955).
- ¹⁷P. C. Samartzis, B. Bakker, T. P. Rakitzis, D. H. Parker, and T. N. Kit-sopoulous, J. Chem. Phys. **110**, 5201 (1999).
- ¹⁸J. W. Hudgens, T. G. DiGiuseppe, and M. C. Lin, J. Chem. Phys. **79**, 571 (1983).
- ¹⁹D. W. Chandler, J. W. Thoman, M. H. M. Janssen, and D. H. Parker, Chem. Phys. Lett. **156**, 151 (1989).
- ²⁰J. Schlüter, R. Schott, and K. Kleinermanns, Chem. Phys. Lett. **213**, 262 (1993).
- ²¹H. M. Kaylor and A. H. Nielsen, J. Chem. Phys. **23**, 2139 (1955).
- ²²J. C. Corchado, D. G. Truhlar, and J. Espinosa-Garcia, J. Chem. Phys. **112**, 9375 (2000).
- ²³W. J. van der Zande, R. Zhang, R. N. Zare, K. G. McKendrick, and J. J. Valentini, J. Phys. Chem. **95**, 8205 (1991).
- ²⁴Q.-S. Xin and X.-Y. Zhu, J. Chem. Phys. **104**, 8829 (1996).